

# Guanine-based amphiphiles: synthesis, ion transport properties and biological activity

Domenica Musumeci,<sup>[a]</sup> Carlo Irace,<sup>[b]</sup> Rita Santamaria,<sup>[b]</sup> Domenico Milano,<sup>[c]</sup> Paolo Tecilla,<sup>[c]</sup> and Daniela Montesarchio<sup>[a]\*</sup>

[a] Dr. Domenica Musumeci, prof. Daniela Montesarchio,  
Department of Chemical Sciences,  
University Federico II of Napoli, Via Cintia, 4, I-80126 Napoli, Italy  
Fax: (+) +39-081-674393, E-mail: [daniela.montesarchio@unina.it](mailto:daniela.montesarchio@unina.it)

[b] Dr. Carlo Irace, prof. Rita Santamaria,  
Department of Pharmacy, University Federico II of Napoli, Via D. Montesano, 49, I-80131  
Napoli, Italy

[c] Dr. Domenico Milano, prof. Paolo Tecilla,  
Department of Chemical Sciences, University of Trieste, Via L. Giorgieri, I-34127 Trieste,  
Italy

**Abstract.** Novel amphiphilic guanine derivatives, here named **Gua1** and **Gua2**, have been prepared through few, simple and efficient synthetic steps. In ion transport experiments through phospholipid bilayers, carried out to evaluate their ability to mediate H<sup>+</sup> transport, **Gua2** showed high activity. When this compound was investigated for ion-selective transport activities, no major differences were observed in the behaviour with cations while, in the case of anions, selective activity was observed in the series I<sup>-</sup>>Br<sup>-</sup>>Cl<sup>-</sup>>F<sup>-</sup>. The bioactivity of these guanine analogues has been evaluated on a panel of human tumour and non-tumour cell lines in preliminary *in vitro* cytotoxicity assays, showing a relevant antiproliferative profile for **Gua2**.

**Keywords:** guanine derivatives; amphiphiles; synthetic ionophores; *in vitro* bioactivity tests.

## Introduction

Among the canonical nucleobases, guanine plays a special role, having an extraordinary ability to produce multiple hydrogen bonds and thus generate not only Watson-Crick interactions but also a variety of non-Watson-Crick specific recognition schemes [1]. Thus, either in the form of single base or nucleoside, or incorporated in guanine-rich oligonucleotides, guanine derivatives may result into higher order self-assembling arrangements, such as the G-quadruplex structures, which are complex three-dimensional architectures consisting of stacked G-tetrads stabilized by Na<sup>+</sup> or K<sup>+</sup> cations [2-4].

As a general remark, the biological activity of guanines and guanosines is not only related to their incorporation into specific DNA and/or RNA sequences, but can be found also in single nucleosides/nucleotides and/or nucleoside analogues. The stringent need for effective antiviral drugs has been the main trigger for the research in the field of nucleoside analogues in the last three decades. These efforts have produced a plethora of new, diverse compounds, many of which endowed with relevant bioactivity [5,6]. Well known examples of antiviral modified guanosines are acyclovir [7], ganciclovir [8] and entecavir [9], which are currently adopted in clinic against HSV,

CMV and HBV, respectively. In more recent years, the interest for nucleoside analogues has been rekindled also in the frame of a general revisitation of their potential as anticancer and antibacterial agents [10-14].

We recently described some amphiphilic guanosine analogues as model compounds of a still very poorly investigated class of guanosine derivatives [15]. Our basic idea was to contribute to “bridging the gap” – in terms of knowledge and applications - between naturally occurring hydrophilic guanosine-based compounds (nucleotides and their congeners), on one side, and artificial lipophilic derivatives, on the other, emerged as promising nanotechnological tools. In order to produce a small library of different amphiphilic derivatives, we elaborated a simple, general synthetic procedure to introduce various lipophilic and hydrophilic appendages at the ribose moiety, so to ensure the highest molecular diversity within very straightforward synthetic schemes. Studies on the ability of the synthesized compounds to transport ions through phospholipids bilayers showed interesting results in the case of compounds **G5**, **G6** and **G7** (Figure 1), which well correlated with their cytotoxicity on several human tumour cell lines.

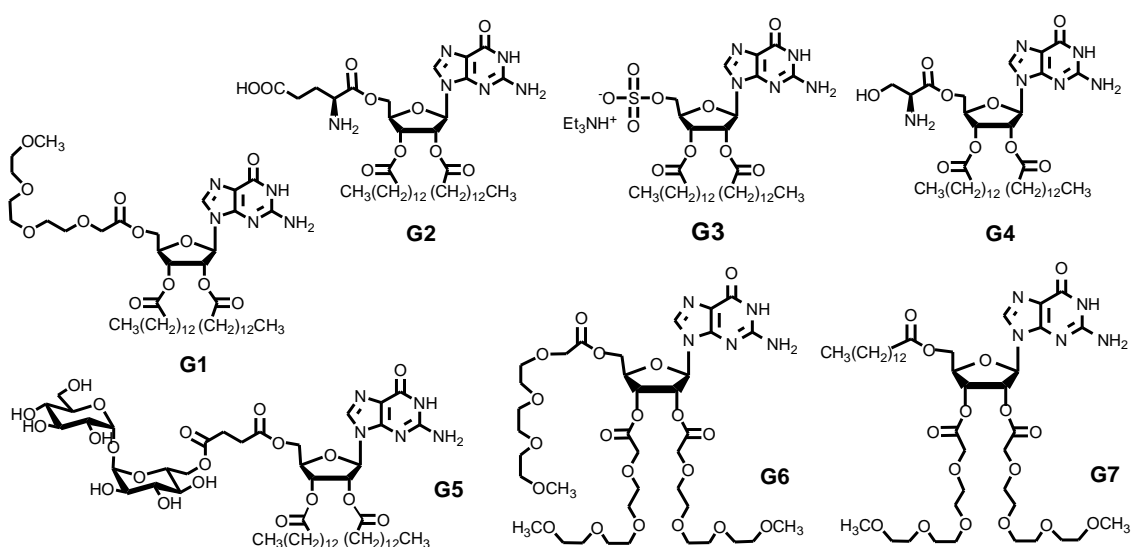


**Figure 1.** Chemical structures of the amphiphilic derivatives of guanosine previously studied in our group [15].

These encouraging results prompted us to further expand the repertoire of amphiphilic guanosine derivatives to obtain optimized compounds with improved ionophore and/or antiproliferative activity. In this work, we report the synthesis and characterization of two novel guanine analogues, which, compared with the previously described derivatives, have simplified structures, lacking the ribose moiety and exhibiting a single structural motif directly attached to the nucleobase. Their ion transport ability through phospholipid membranes, as well as preliminary *in vitro* data on their antiproliferative activity on tumour and non tumour cell lines are also presented.

## Results and Discussion

### Chemistry.

Intrigued by optimization processes in drug discovery aimed at screening extremely simplified structures, we have synthesized two novel derivatives, **Gua1** and **Gua2**, depicted in Figure 2, as model compounds of a novel family of amphiphiles. These analogues share a common design, based on the derivatization of the N9 position of the guanine moiety with a single hydrophilic structural motif, resulting into differently decorated ribose-free species.

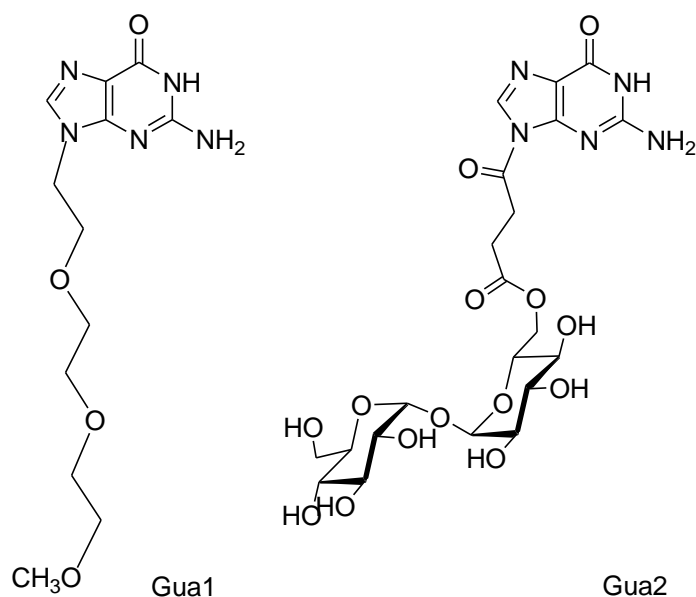


**Figure 2.** Chemical structures of the amphiphilic guanine derivatives studied in this work.

The structural requirements explored in the design of **Gua1** and **Gua2** satisfy a general principle of atom economy and have been inspired by a recent work, in which high ion transport activity through lipid membranes has been found in a very simple construct, consisting of a benzothiazole-aniline core functionalized with a single tetraethylene glycol chain [16]. Assuming that this heteroaromatic compound can be effectively replaced by a guanine residue, the insertion of hydrophilic groups at its N9 position should then add the overall polarity necessary to obtain an amphiphilic derivative, with sufficient water solubility and able to interact with lipid bilayers.

In **Gua1** and **Gua2** a triethylene glycol chain and a trehalose residue, respectively, have been inserted into the guanine scaffold; these polar appendages have been selected on the basis of our previous data on amphiphilic guanosine derivatives, showing **G5** and **G6** (Figure 1), incorporating these structural motifs, as the most active compounds [15].

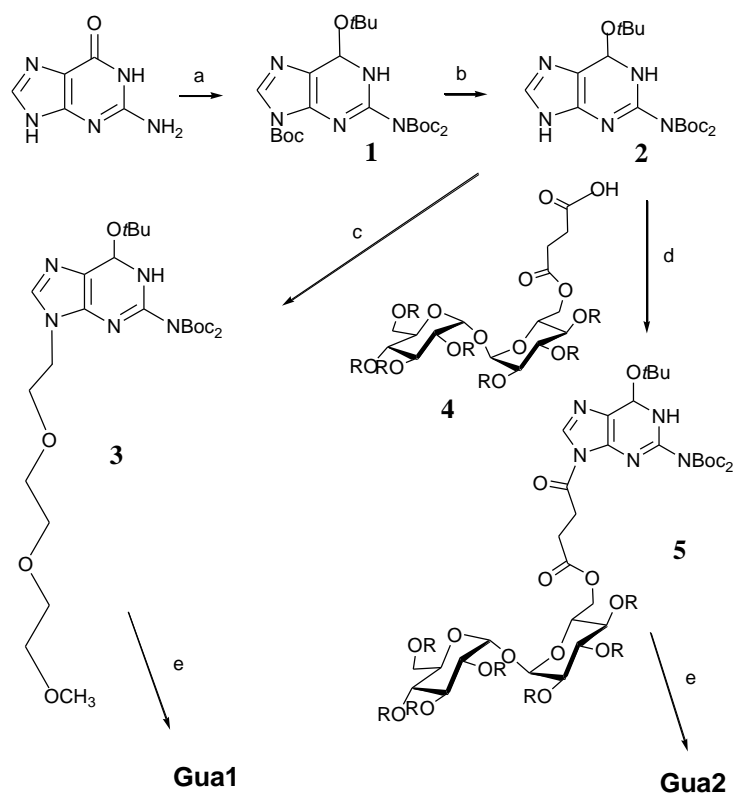
The target derivatives **Gua1** and **Gua2** have been obtained through a straightforward, flexible and efficient procedure, using a partially protected guanine building block as a common intermediate (**2**, Scheme 1). This was prepared from guanine in two simple steps, involving first the reaction with an excess of Boc anhydride in the presence of cat. DMAP, which gave the fully protected nucleobase **1** [17]. Then the treatment with a satd NaHCO<sub>3</sub> solution, essentially following a published procedure [18], allowed to selectively remove the Boc group at the N9 position. The resulting guanine derivative **2** was thus exploited in the coupling with either monomethoxytriethylene glycol, exposing a free primary alcohol group, or a fully Boc-protected trehalose monosuccinic acid derivative, synthesized as previously described [15] and exposing a COOH group (**4**, Scheme 1). In the first case the coupling was realized *via* a Mitsunobu reaction, in the latter *via* a standard DCC activation of the carboxylic function.

Monomethoxytriethylene glycol, used for the synthesis of **Gua1**, is commercially available and has been coupled as such with protected guanine **2** using triphenylphosphine and DIAD as condensing agents in anhydrous THF. Target derivative **3** has been thus obtained in 90% yields after purification.

For the synthesis of **Gua2**, guanine derivative **2** has been coupled with the disaccharide building block **4** in the presence of DCC/DMAP in anhydrous CH<sub>2</sub>Cl<sub>2</sub>, giving **5** in 95% yields after column chromatography. Following a previously described procedure, the used disaccharide **4** has been obtained in few, simple reactions starting from  $\alpha,\alpha'$ -D-trehalose. This is a symmetrical disaccharide widely represented in nature, having a peculiar ability to stabilize phospholipid membranes [19]. In addition it offers many favourable features in terms of synthetic manipulations, since it is a non-

reducing sugar, does not undergo mutarotation, and its O-glycosidic bond is pretty stable compared to other disaccharides [20,21]. The latter issue is of the utmost relevance considering that preformed disaccharides are privileged scaffolds for the synthesis of glyco-peptides, glyco-oligonucleotides or other hybrid compounds, but typically the acidic treatments required for the oligomer deprotection steps prevent their use and thus suitable glycomimetics have to be designed. Typically, these saccharide-based building blocks are obtained through several synthetic steps and are protected on the OH groups with base-labile acetyl groups [22-24]. In this strategy, the use of trehalose derivative **4**, fully protected with acid-labile Boc groups, has allowed a unique protection scheme for adduct **5** so that target compound **Gua2** can be obtained in a pure form through a single deprotection step.

Clean removal of both Boc and *t*Bu groups has been achieved treating the protected adducts **3** and **5** with 10% TFA in anhydrous CH<sub>2</sub>Cl<sub>2</sub>, which gave the corresponding fully deprotected compounds in almost quantitative yields. Final compounds **Gua1** and **Gua2**, as well as all the synthesized intermediates, have been fully characterized by <sup>1</sup>H and <sup>13</sup>C NMR and MS analysis.



**Scheme 1.** Synthesis of **Gua1** and **Gua2**. Reaction conditions: a) Boc<sub>2</sub>O, DMAP, TEA, CH<sub>3</sub>CN, 4 d, r.t., 51% yields; b) NaHCO<sub>3</sub> satd. soln. in CH<sub>3</sub>OH, 1 h, 50 °C, 96% yields; c) CH<sub>3</sub>O(CH<sub>2</sub>CH<sub>2</sub>O)CH<sub>2</sub>CH<sub>2</sub>OH, PPh<sub>3</sub>, DIAD; THF, 12 h, r.t. 90%; d) Boc-protected trehalose 6-monosuccinic acid (**4**), DCC, DMAP, 30 min, r.t., 95%; e) 10% TFA in CH<sub>2</sub>Cl<sub>2</sub>, 2 h, r.t., quant. R = Boc.

### Ion transport studies through lipid membranes.

The ionophoric activity of compounds **Gua1** and **Gua2** has been investigated in large unilamellar vesicles (100 nm diameter, prepared by extrusion) with a 95:5 egg phosphatidylcholine (EYPC) and egg phosphatidylglycerol (EYPG) lipid composition.

The ability of the ionophore to mediate a pH gradient collapse across the membrane has been measured using the pH-sensitive fluorescent dye HPTS (HPTS = 8-hydroxypyrene-1,3,6-trisulfonic acid, pK<sub>a</sub> = 7.2). In this assay the dye is entrapped inside the phospholipid vesicles prepared in

HEPES buffer (pH 7.0) containing 100 mM NaCl and, after addition of the ionophore, a pH gradient of 0.6 pH units is applied by external addition of NaOH. The collapse of this transmembrane pH-gradient implies basification of the liposome inner water pool, which is signalled by an increase of the HPTS fluorescence emission. Therefore, the rate of the pH gradient collapse gives direct information on the transportation of OH<sup>-</sup> (influx) or H<sup>+</sup> (efflux) and indirect information on the correlated symport/antiport of counterions required to counterbalance the transmembrane ions movement. Figure 3a shows the typical kinetic profiles obtained upon addition of NaOH at 200 s and lyses of the liposomes by addition of Triton X-100 at 1400 s.

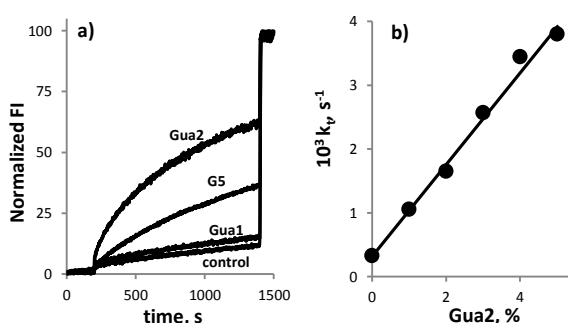


**Figure 3.** a) Normalized fluorescence change in HPTS emission as a function of time after addition of the base (50  $\mu$ L of 0.5 M NaOH) to 95:5 EYPC/EYPG LUVs (100 nm diameter) loaded with HPTS (0.1 mM HPTS, 0.17 mM total lipid concentration, 25 mM HEPES, 100 mM NaCl, pH 7.0), in the presence of 2% concentration of **Gua1**, **Gua2**, and **G5**. The concentration of the ionophores is given in percent with respect to the total lipid concentration. The control trace has been recorded in the absence of ionophore. (b) Plot of the observed rate constant for the transport process ( $k_t$ , s<sup>-1</sup>) vs concentration for ionophore **Gua2**.

Of the two guanine derivatives here investigated, only **Gua2** shows interesting ionophoric activity while **Gua1** is substantially inactive. Remarkably, **Gua2** is about two times more active than **G5**, that was the most efficient ionophore within the previous series investigated ([15], Figure 1). This result suggests that the guanine nucleus and the trehalose subunit are essential, while the ribose moiety is not required, or even detrimental, for ionophoric activity. Control experiments, carried out separately on guanine and trehalose as isolated compounds, showed no activity (see Supplementary Content, Figure S1). Similar results were obtained also analysing the lipophilic derivative 6-*tert*-butyldiphenylsilyl-trehalose [15], which is a monoprotected derivative of trehalose having similar polarity as **Gua2**, obtained as precursor of 6-monosuccinylated derivative **4**. Even if this compound proved to be slightly more active than trehalose alone – see Figure S1, panel c – its effects are largely marginal in comparison with **Gua2**. Taken together, all these results converge in concluding that it's the proper combination of structural motifs in **Gua2** – the nucleobase and the disaccharide – responsible for the observed activity.

On the other hand, the hydrophilic portion of **Gua1** is probably too small and the compound is not able to permeabilize the phospholipid bilayer. A strong correlation between the size of the hydrophilic portion and the ionophoric activity has been indeed observed in the previous investigated series of guanosine derivatives as well as in somehow structurally related CyPLOS derivatives [25,26].

The activity of **Gua2** depends on its concentration as shown in Figure 3b, which reports the observed pseudo-first-rate constants obtained by fitting the kinetic profiles recorded in the conditions of Figure 3a and in the presence of increasing concentrations of ionophore. The dependence of the rate constant from the concentration of **Gua2** is linear, suggesting that the active species responsible for the transport process is monomeric. Interestingly, kinetic experiments performed in the conditions of Figure 3a but in the presence of K<sup>+</sup> instead of Na<sup>+</sup> indicate that the ionophoric activity of the two guanine derivatives is not influenced by the cation present in solution

(see also below) suggesting that, as already observed with the guanosine derivatives of Figure 1, the potassium cation is not able to promote the assembly of guanine aggregates in membranes. This result confirms that simple guanine derivatives are not suitable to form G-quartet structures in phospholipid membranes under the studied concentration conditions, as conversely already observed with more complex guanosine-based systems [27,28]. To further exclude possible aggregation events occurring in solution when investigating **Gua1** and **Gua2** alone, or in the membrane when mixed with the examined phospholipids, DLS measurements have been carried out (see Supplementary Content). In the case of the isolated ionophores, analyzed at  $\mu\text{M}$  concentrations, no aggregates could be observed, demonstrating that both **Gua1** and **Gua2** do not tend to form supramolecular structures detectable under the used experimental set-up. Then, when mixed with the 95:5 EYPC/EYPG phospholipid at 2% mol/mol ratio, the size and morphology of the resulting aggregates were in no case sensibly altered.

Selectivity in ion transport for **Gua2** has been investigated with the HPTS assay using the protocol described above and in the presence of HEPES buffer containing the cation or the anion under investigation added as MCl or NaX salt, respectively [29]. The obtained results show similar transport rates in the presence of the first group alkali metals (Figure 4a) and a strong dependence on the nature of the halide present, with transport rates increasing from fluoride to iodide (Figure 4b). Independence of the transport process from the nature of the cation and dependence from the nature of the anion is an evidence that the basification of the inner vesicular water pool signaled by HPTS correlates with  $\text{OH}^-/\text{X}^-$  antiport (or to the kinetically equivalent  $\text{H}^+/\text{X}^-$  symport). Accordingly, the kinetic traces of Figure 4a report on the transport of chloride which is present as the common counterion of all the cations used in this set of experiments. On the other hand, the selectivity sequence observed in the transport of halides follows the lyotropic series, with the less hydrated ions transported faster than the more hydrated ones. Therefore, the transport process appears governed by the translocation of the anion and rate-limited by the cost of its dehydration.

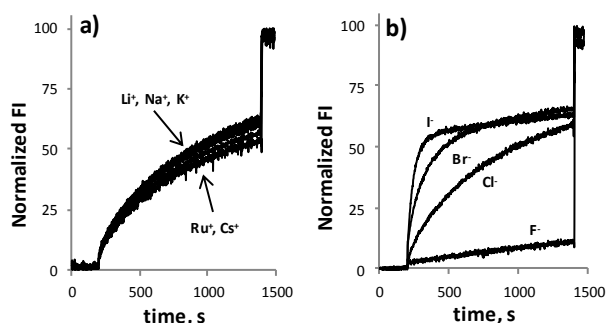


**Figure 4.** a) Cation selectivity of **Gua2** (2 %) determined by the HPTS assay (MCl (100 mM), pH 7.0, base pulse by addition of MOH (50  $\mu\text{L}$ , 0.5 M)). b) Anion selectivity of **Gua2** (2 %) determined by the HPTS assay (NaX (100 mM), pH 7.0, base pulse by addition of NaOH (50  $\mu\text{L}$ , 0.5 M)). The kinetics were corrected for spontaneous permeation of the different anions. Other conditions as specified in Figure 3.

The inactivity of **Gua1** and the activity and ion selectivity of **Gua2** compare well with the ionophoric behavior observed with the guanosine derivatives **G1-G7** and we therefore propose the same mechanism of action for these structurally related compounds. In this model, **Gua2** inserts in the membrane with the guanine moiety anchored on the surface and the trehalose subunit dipped in the phospholipid bilayer. The effect of the polar sugar is a destabilization of the membrane with the formation of disordered patches, characterised by an increased permeability which allows the transit of the ions in a process mainly governed by the cost of the anion dehydration. Interestingly, removal of the ribose moiety between the nucleobase and the trehalose results in an increase of activity, probably related to a better insertion mode of the ionophore in the membrane due to steric factors or to a more favourable hydrophilic/hydrophobic balance.

### ***In vitro* bioscreenings for cytotoxic activity.**

Although several amphiphiles based on canonical nucleobases are described in the literature, very few examples are known for guanine derivatives and their potential in biomedical applications is almost completely unexplored. In this frame, our group recently showed that guanosine-based systems are endowed with biological/biomedical potential, displaying an interesting antiproliferative activity towards certain types of human cancer cells not directly related to their DNA and RNA-targeting properties [15]. These findings prompted us to test **Gua1** and **Gua2** for cytotoxic activity on a selected panel of human cell lines. Bioscreenings are useful *in vitro* assays to validate a particular bioactivity and the herein reported experimental procedure allows the estimation of the cytotoxicity by a “cell survival index” determined by monitoring the cellular metabolic activity and the live/dead cells ratio. The results are reported both in concentration-effect curves (Figure 5) and in terms of IC<sub>50</sub> values (Table 1). Data concerning cisplatin (cDDP) - a positive control for cytotoxic activity - are included for comparison.

The most important outcome emerging from these assays is that **Gua2** exhibits a considerable bioactivity pattern characterized by a non-selective cytotoxicity against human cancer and non-cancer cell lines of different histological origins. The corresponding IC<sub>50</sub> values, ranging in the low micromolar range, are comparable to those found for cisplatin and are consistent with a moderate-to-strong cytotoxic effect. Indeed, in HaCaT and MCF-7 the **Gua2** effects on cell growth are even more pronounced than those of cisplatin. Conversely, in all cases **Gua1** shows IC<sub>50</sub> values >10<sup>2</sup> μM, without causing any apparent effect on cell viability and/or proliferation.

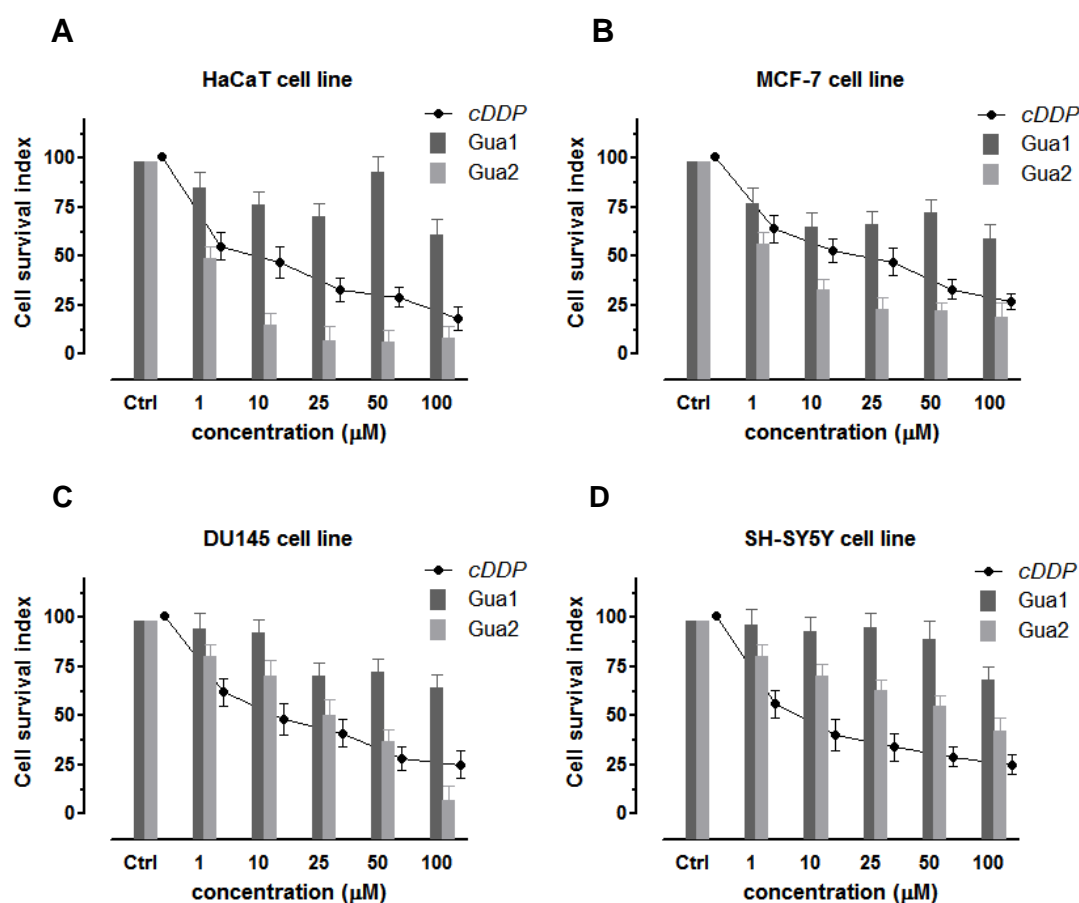


**Figure 5.** Cell survival index values, evaluated by MTT assay and total cell count, in HaCaT (panel A), MCF-7 (panel B), DU145 (panel C) and SH-SY5Y (panel D) cell lines incubated for 48 h with a range of concentrations (1→100 μM) of **Gua1** and **Gua2** (color bars) and with cisplatin (cDDP, solid line), here used as positive control for cytotoxicity. Data are expressed as percentage of untreated control cells and are reported as mean of four independent experiments ± SEM.

**Table 1** - IC<sub>50</sub><sup>a</sup> values (μM) for **Gua1** and **Gua2** in the indicated cell lines following 48 h of incubation. Positive control for cytotoxicity was performed using cisplatin (*cDDP*).

<i>Cell lines</i>	<i>cDDP</i>	<i>Gua1</i>	<i>Gua2</i>	<i>G5<sup>b</sup></i>
<b>HaCaT</b>	7 ± 2.5	> 10 <sup>2</sup>	1 ± 0.8	n.d.
<b>MCF7</b>	25 ± 4	> 10 <sup>2</sup>	5 ± 2	17 ± 5 <sup>b</sup>
<b>DU145</b>	20 ± 5	> 10 <sup>2</sup>	25 ± 3	n.d.
<b>SH-SY5Y</b>	2 ± 0.9	> 10 <sup>2</sup>	80 ± 5	n.d.

<sup>a</sup> IC<sub>50</sub> values are reported as mean ± SEM (*n* = 24) of 3 independent experiments; <sup>b</sup> data from ref. 15; n.d. = not determined.

## Conclusions.

In this work we have described the synthesis and characterization of two new guanine analogues, respectively conjugated with an oligoethylene glycol chain and a trehalose residue, proposed as model compounds of a new family of easily synthetically accessible amphiphiles. An efficient and versatile synthetic scheme has been adopted for their preparation, involving a partially protected guanine derivative as a common intermediate, able to react at the sole N9 position either with alcohols, *via* a Mitsunobu procedure, or with carboxylic acids, *via* standard DCC activation. After coupling, in both cases the target compounds have been obtained through a single acidic deprotection step. This synthetic strategy has been particularly efficient in the case of the disaccharide-conjugated derivative **Gua2**, realized using the valuable fully Boc-protected trehalose building block **4**, of interest in a variety of glyco-conjugations.

**Gua1** and **Gua2**, analyzed in their ability to transport ions through lipid bilayers, showed a very different behaviour. High activity has been observed only in the latter compound, having also a marked specificity in the transport of anions, thus indicating that the polar appendage attached to the nucleobase is the most relevant structural motif for this property. In comparison with the previously investigated guanosine derivatives [15], **Gua2** is about two times more efficient than the corresponding trehalose-containing derivative **G5**. Therefore, the proposed structural simplification approach turned out to be successful in producing enhanced ionophoric activity.

The bioactivity of these new compounds has been investigated on a panel of human cancer and healthy cells. Preliminary data showed that **Gua1** has a negligible antiproliferative profile, while remarkable *in vitro* activity – higher than that of cisplatin, here used as a reference compound - has been found in **Gua2** when tested against human MCF-7 and HaCaT cell lines.

Thus, in line with previous studies, carried out by us [15] and others [30], remarkably the anionophoric activity of the tested compounds has been found to well correlate with their *in vitro* bioactivity.

If in general no straightforward cause-effect relationship can be invoked to exist between ion transport properties and cytotoxicity of small molecules, these results suggest that anion transport might play a significant role in the mechanism of action of these compounds in cell. In fact, it is known that the anion transport can influence the sophisticated mechanisms of regulation of intracellular pH by determining changes that can trigger apoptosis [31]. Thus, the search for structural motifs ensuring improved anion transport abilities could be extremely helpful in the rational design of novel optimized drugs with a more favourable pharmacological profile.

Starting from the promising data on **Gua2**, our future studies in this field will be addressed to investigate a larger set of guanine analogues, aiming at obtaining more specific bioactive compounds.



## Experimental Section.

### General Methods.

All the reagents were of the highest commercially available quality and were used as received. TLC analyses were carried out on silica gel plates from Merck (60, F254). Reaction products on TLC plates were visualized by UV light and then by treatment with a 10 %  $\text{Ce}(\text{SO}_4)_2/\text{H}_2\text{SO}_4$  aqueous solution. For column chromatography, silica gel from Merck (Kieselgel 40, 0.063-0.200 mm) was used. NMR spectra were recorded on Varian Gemini 200 and Varian Inova 500 spectrometers, as specified. All the chemical shifts are expressed in ppm with respect to the residual solvent signal. Peak assignments have been carried out on the basis of standard H-H COSY and HSQC experiments. For the ESI MS analyses, a Waters Micromass ZQ instrument – equipped with an Electrospray source – was used in the positive mode. MALDI TOF mass spectrometric analyses were performed on a PerSeptive Biosystems Voyager-De Pro MALDI mass spectrometer in the Linear mode.

### Abbreviations.

The following abbreviations have been used throughout the text: AcOEt = ethyl acetate; Boc = *tert*-butoxycarbonyl; Boc<sub>2</sub>O = Boc anhydride; DCC = dicyclohexylcarbodiimide; DIAD = diisopropylazodicarboxylate; DMAP = 4-(*N,N*-dimethylamino)pyridine; DMF = *N,N*-dimethylformamide; PPh<sub>3</sub> = triphenylphosphine; *t*Bu = *tert*-butyl; TEA = triethylamine; TFA = trifluoroacetic acid; THF = tetrahydrofuran.

### Synthesis of fully protected triethylene glycol derivative **3**.

Partially protected guanine derivative **2** (40 mg, 0.098 mmol), synthesized from guanine in two steps [17,18], and monomethoxytriethylene glycol (33  $\mu\text{L}$ , 34 mg, 0.21 mmol) were dissolved under stirring in anhydrous THF (3.0 mL) and the resulting mixture was then treated with PPh<sub>3</sub> (54 mg, 0.21 mmol) and DIAD (41  $\mu\text{L}$ , 42 mg, 0.21 mmol) at r.t. After 12 h, TLC monitoring showed the complete disappearance of the guanine-containing starting material and the formation of a unique new compound. The reaction mixture was then taken to dryness under reduced pressure and the residue, redissolved in AcOEt, was then applied to a silica gel column, eluted with *n*-hexane/AcOEt (1:9, v/v). Collection of the appropriate fractions gave pure target compound **3** (49 mg, 0.088 mmol), obtained in 90% yield.

**3**: oil.  $R_f$  = 0.5 in AcOEt. <sup>1</sup>H NMR (200 MHz, CDCl<sub>3</sub>)  $\delta$  at: 8.07 (s, 1H, H-8); 4.38 (apparent t,  $J$  = 4.8 and 5.0 Hz, 2H, CH<sub>2</sub>OCH<sub>3</sub>); 3.78 (apparent t,  $J$  = 4.8 and 5.0 Hz, 2H, CH<sub>2</sub>CH<sub>2</sub>N); 3.45-3.38 (overlapped signals, 8H, 2x CH<sub>2</sub>OCH<sub>2</sub>); 3.36 (s, 3H, OCH<sub>3</sub>); 1.70 (s, 9H, *t*Bu); 1.39 (s, 18H, 2x Boc). <sup>13</sup>C NMR (50 MHz, CDCl<sub>3</sub>)  $\delta$  at: 161.2 (C6); 152.8 (C2); 151.7 (C4); 150.8 (CO Boc); 141.2 (C8); 121.6 (C5); 84.4 (quaternary C of *t*Bu); 82.9 (quaternary C of Boc); 71.6, 71.3, 70.1, 68.5 and 68.3 (5x CH<sub>2</sub>O); 59.1 (OCH<sub>3</sub>); 46.6 (CH<sub>2</sub>N); 28.3 (CH<sub>3</sub> groups of *t*Bu); 27.9 (CH<sub>3</sub> groups of Boc). ESI-MS (positive ions): for C<sub>26</sub>H<sub>43</sub>N<sub>5</sub>O<sub>8</sub>, calcd. 553.31; found  $m/z$ : 554.61 [M+H<sup>+</sup>, 25%]; 576.72 [M+Na<sup>+</sup>, 100%]; 592.79 [M+K<sup>+</sup>, 30%]. HRMS (MALDI-TOF): calcd. for C<sub>26</sub>H<sub>43</sub>N<sub>5</sub>O<sub>8</sub>Na = 576.3009; found  $m/z$ : 576.3021 [M + Na<sup>+</sup>].

### Synthesis of **Gua1**.

Fully protected derivative **3** (25 mg, 0.045 mmol) was left in contact with a 10% TFA solution in anhydrous CH<sub>2</sub>Cl<sub>2</sub> (1.0 mL) at r.t. under stirring. After 2 h, TLC monitoring showed the complete disappearance of the starting material and formation of a unique new compound. The reaction mixture was then diluted with CH<sub>2</sub>Cl<sub>2</sub>, taken to dryness under reduced pressure and the residue coevaporated several times with 2-propanol, affording pure **Gua1** (13 mg, 0.045 mmol) in almost quantitative yields.

**Gua1:** oil.  $R_f = 0.2$  in AcOEt.  $^1\text{H}$  NMR (200 MHz,  $\text{CD}_3\text{OD}$ )  $\delta$  at: 9.00 (s, 1H, H-8); 4.41 (t,  $J = 4.8$  and 4.8 Hz, 2H,  $\text{CH}_2\text{OCH}_3$ ); 3.86 (apparent t,  $J = 4.8$  and 5.0 Hz, 2H,  $\text{CH}_2\text{CH}_2\text{N}$ ); 3.64-3.48 (overlapped signals, 8H, 2x  $\text{CH}_2\text{OCH}_2$ ); 3.34 (s, 3H,  $\text{OCH}_3$ ).  $^{13}\text{C}$  NMR (50 MHz,  $\text{CD}_3\text{OD}$ )  $\delta$  at: 157.2 (C6); 155.4 (C2); 151.7 (C4); 139.1 (C8); 115.3 (C5); 71.5, 71.2, 70.0, 68.4 and 68.2 (5x  $\text{CH}_2\text{O}$ ); 59.1 ( $\text{OCH}_3$ ); 46.5 ( $\text{CH}_2\text{N}$ ). ESI-MS (positive ions): for  $\text{C}_{12}\text{H}_{19}\text{N}_5\text{O}_4$ , calcd. 297.14; found  $m/z$ : 298.54 [ $\text{M}+\text{H}^+$ , 21%]; 320.64 [ $\text{M}+\text{Na}^+$ , 100%]; 336.71 [ $\text{M}+\text{K}^+$ , 36%]. HRMS (MALDI-TOF): calcd. for  $\text{C}_{12}\text{H}_{19}\text{N}_5\text{O}_4\text{Na} = 320.1335$ ; found  $m/z$ : 320.1361 [ $\text{M} + \text{Na}^+$ ].

#### *Synthesis of fully protected trehalose derivative 5.*

Partially protected guanine derivative **2** (8.0 mg, 0.020 mmol) and Boc-protected trehalose 6-monosuccinic acid **4** (24 mg, 0.021 mmol), synthesized as previously described [15]. were dissolved under stirring in anhydrous  $\text{CH}_2\text{Cl}_2$  (1.0 mL) in the presence of DCC (6.0 mg, 0.03 mmol) and DMAP (0.2 mg, 0.002 mmol). After 30 min at r.t. TLC monitoring showed the complete disappearance of the starting materials and the formation of a unique new compound. The reaction mixture was then taken to dryness under reduced pressure and the residue, redissolved in AcOEt, was then applied to a silica gel column, eluted with *n*-hexane/AcOEt (3:2, v/v). Collection of the appropriate fractions gave pure target compound **5** (29 mg, 0.019 mmol), obtained in 95% yield.

**5:** amorphous solid.  $R_f = 0.7$  in *n*-hexane/AcOEt (1:1, v/v).  $^1\text{H}$  NMR (500 MHz,  $\text{CDCl}_3$ )  $\delta$  at: 8.57 (s, 1H, H-8); 5.25 (apparent t,  $J = 3.5$  and 3.5 Hz, overlapped signals, 2H, H-1' and H-1''); 5.21 (overlapped signals, 2H, H-3' and H-3''); 5.01-4.94 (overlapped signals, 2H, H-4' and H-4''); 4.90-4.85 (overlapped signals, 2H, H-2' and H-2''); 4.43-4.40 (m, 1H,  $\text{H}_a\text{-6'}$ ); 4.39-4.36 (m, 1H,  $\text{H}_a\text{-6''}$ ); 4.32-4.23 (overlapped signals, 2H, H-5' and H-5''); 4.08-4.07 (m, 1H,  $\text{H}_b\text{-6'}$ ); 4.01-3.98 (m, 1H,  $\text{H}_b\text{-6''}$ ); 3.68 (m, 2H,  $\text{CH}_2$  succinic residue); 2.87 (t,  $J = 6.0$  and 6.0 Hz, 2H,  $\text{CH}_2$  succinic residue); 1.72 (s, 9H, *t*Bu); 1.49, 1.48, 1.47, 1.46, 1.45, 1.44 and 1.43 (s's, 9H each, 7x Boc); 1.31 and 1.29 (s's, 9H each, 2x Boc).  $^{13}\text{C}$  NMR (125 MHz,  $\text{CDCl}_3$ )  $\delta$  at: 171.6 and 169.5 (CO of the succinic ester and amide); 161.3 (C6); 153.2 (C2); 152.0 and 151.1 (CO of the Boc groups); 150.7 (C4); 138.8 (C8); 121.8 (C5); 94.5 (C-1', C-1''); 84.7 (quaternary C of *t*Bu), 83.2, 83.0, 82.8, 82.5, 82.2 (quaternary C of the Boc groups); 73.0 (C-3', C-3''); 72.1 (C-2', C-2''); 70.4 (C-4', C-4''); 68.1 (C-5', C-5''); 63.3 (C-6'); 61.6 (C-6''); 55.7 ( $\text{CH}_2$  succinic residue); 28.2 ( $\text{CH}_3$  groups of *t*Bu), 27.8, 27.7, 25.4 and 24.7 ( $\text{CH}_3$  groups of Boc). ESI-MS (positive ions): for  $\text{C}_{70}\text{H}_{109}\text{N}_5\text{O}_{32}$ , calcd. 1531.71; found  $m/z$ : 1532.11 [ $\text{M}+\text{H}^+$ , 27%]; 1554.21 [ $\text{M}+\text{Na}^+$ , 100%]; 1571.10 [ $\text{M}+\text{K}^+$ , 46%]. HRMS (MALDI-TOF): calcd. for  $\text{C}_{70}\text{H}_{109}\text{N}_5\text{O}_{32}\text{Na} = 1554.6953$ ; found  $m/z$ : 1554.6979 [ $\text{M} + \text{Na}^+$ ].

#### *Synthesis of Gua2.*

Fully protected derivative **5** (25 mg, 0.016 mmol) was left in contact with a 10% TFA solution in anhydrous  $\text{CH}_2\text{Cl}_2$  (1.0 mL) at r.t. under stirring. After 2 h, TLC monitoring showed the complete disappearance of the starting material and the formation of a unique new compound. The reaction mixture was then diluted with  $\text{CH}_2\text{Cl}_2$ , taken to dryness under reduced pressure and the residue coevaporated several times with 2-propanol, affording pure **Gua2** (10 mg, 0.016 mmol) in almost quantitative yields.

**Gua2:** amorphous solid.  $R_f = 0.5$  in AcOEt/ $\text{CH}_3\text{OH}$  (5:1, v/v).  $^1\text{H}$  NMR (400 MHz,  $\text{CD}_3\text{OD}$ ), broad, not well resolved signals with  $\delta$  at: 8.68 (s, 1H, H-8); 5.31 (overlapped signals, 2H, H-1' and H-1''); 5.26 (overlapped signals, 2H, H-3' and H-3''); 5.09-4.98 (overlapped signals, 2H, H-4' and H-4''); 4.93-4.87 (overlapped signals, 2H, H-2' and H-2''); 4.47-4.44 (m, 1H,  $\text{H}_a\text{-6'}$ ); 4.40-4.38 (m, 1H,  $\text{H}_a\text{-6''}$ ); 4.35-4.25 (overlapped signals, 2H, H-5' and H-5''); 4.12-4.10 (m, 1H,  $\text{H}_b\text{-6'}$ ); 4.08-4.02 (m, 1H,  $\text{H}_b\text{-6''}$ ); 3.72 (m, 2H,  $\text{CH}_2$  succinic residue); 2.92 (m, 2H,  $\text{CH}_2$  succinic residue).  $^{13}\text{C}$  NMR (100 MHz,  $\text{CD}_3\text{OD}$ )  $\delta$  at: 174.9 and 168.8 (CO of the succinic ester and amide); 162.0 (C6); 154.4 (C2); 151.6 (C4); 140.6 (C8); 120.2 (C5); 95.7 (C-1', C-1''); 75.6 (C-3', C-3''); 73.6 (C-2', C-2''); 72.4 (C-4', C-4''); 71.7 (C-5', C-5''); 65.3 (C-6'); 63.1 (C-6''); 56.9 ( $\text{CH}_2$  succinic residue). ESI-MS (positive ions): for  $\text{C}_{21}\text{H}_{29}\text{N}_5\text{O}_{14}$ , calcd. 575.17; found  $m/z$ : 576.85 [ $\text{M}+\text{H}^+$ , 100%]; 598.75

[M+Na<sup>+</sup>, 55%]; 614.70 [M+K<sup>+</sup>, 30%]. HRMS (MALDI-TOF): calcd. for C<sub>21</sub>H<sub>29</sub>N<sub>5</sub>O<sub>14</sub>Na = 598.1609; found *m/z*: 598.1640 [M + Na<sup>+</sup>].

### Ionophoric activity.

L- $\alpha$ -phosphatidyl-DL-glycerol sodium salt (EYPG, 20 mg/mL chloroform solution) was purchased from *Avanti Polar Lipids*; egg yolk phosphatidylcholine (EYPC, 100 mg/mL chloroform solution) and 8-hydroxypyrene-1,3,6-trisulfonic acid trisodium salt (HPTS) were from *Sigma*; Triton<sup>®</sup> X-100 and HEPES buffer were from *Fluka*; all salts were of the best grade available from *Aldrich* and were used without further purification.

Liposomes were prepared by extrusion using a 10 mL *Lipex*<sup>TM</sup> Thermobarrel EXTRUDER (*Northern Lipids Inc.*) connected to a thermostatic bath (25°C if not otherwise indicated). The 100 nm polycarbonate membranes were *Nucleopore Track-Etch Membranes* from *Whatman*. Fluorescence spectra were recorded on a *Varian Cary Eclipse* fluorescence spectrophotometer. All fluorimetric measurements were performed at 25 °C. The ionophores concentration is given in percent with respect to the total concentration of lipids. Mother solutions of ionophores were prepared in methanol. Control experiments showed that the amount of methanol added to the vesicular suspension in the different experiments (maximum amount 2.0 % in volume) did not affect the permeability of the membrane.

### HPTS assay.

A mixture of 150  $\mu$ L of EYPC chloroform solution (100 mg/mL, 20  $\mu$ mol) and 40  $\mu$ L of EYPG chloroform solution (20 mg/mL, 1  $\mu$ mol) was first evaporated under Ar-flux to form a thin film and then dried under high vacuum for 3 h. The lipid cake was hydrated in 1.5 mL of 0.1 mM HPTS solution (HEPES 25 mM, 100 mMNaCl, pH 7) for 30 min at 40°C. The lipid suspension was submitted to 5 freeze-thaw cycles (−196°C/40°C) using liquid nitrogen and a thermostatic bath, and then extruded under nitrogen pressure (15 bar) at room temperature (10 extrusions through a 0.1  $\mu$ m polycarbonate membrane).

The LUV suspension was separated from extravesicular dye by size exclusion chromatography (SEC) (stationary phase: pre-packed column *Sephadex*<sup>TM</sup> G-25, mobile phase: HEPES buffer) and diluted with HEPES buffer to give a stock solution with a lipid concentration of 5 mM (assuming 100% of lipids were incorporated into liposomes). 104  $\mu$ L of the lipid suspension were placed in a fluorimetric cell, diluted to 3040  $\mu$ L with the same buffer solution used for the liposome preparation and kept under gently stirring. The total lipid concentration in the fluorimetric cell was 0.17 mM. An aliquot of solution of the ionophore in MeOH (10-50  $\mu$ L of the appropriate mother solution in order to obtain the desired mol<sub>compound</sub>/mol<sub>lipid</sub> ratio) was then added to the lipid suspension and the cell was incubated at 25°C for 10 min.

After incubation the time course of the fluorescence emission was recorded for 200 s ( $\lambda_{ex1}$ =460 nm,  $\lambda_{ex2}$ = 403 nm,  $\lambda_{em}$ = 510 nm) and then 50  $\mu$ L of 0.5 M NaOH were rapidly added through an injector port and the fluorescence emission was recorded for 1200 s. Maximal changes in dye emission were obtained by final lysis of the liposomes with a detergent (40  $\mu$ L of 5% aqueous Triton<sup>®</sup> X-100). The data set consists of emission intensities at 510 nm modulated by alternating excitation at 403 nm and 460 nm on a 0.5+0.5 s cycle. The concentration of the conjugate base form of HPTS is related to the emission intensity at 510 nm during the period in which the dye is excited at 460 nm ( $E_{460}$ ) while the concentration of the protonated form is related to the emission intensity at 510 nm during the period in which the dye is excited at 403 nm ( $E_{403}$ ). Fluorescence time courses were normalized using the following equation, where the subscripts 0,  $\infty$  and  $t$  denote the emission ratio before the base pulse, after detergent lysis, and at an intermediate time, respectively.

$$FI = \frac{\left(\frac{E_{403}}{E_{460}}\right)_t - \left(\frac{E_{403}}{E_{460}}\right)_0}{\left(\frac{E_{403}}{E_{460}}\right)_\infty - \left(\frac{E_{403}}{E_{460}}\right)_0} \times 100$$

#### *Determination of cation and anion selectivity with the HPTS assay.*

The vesicle suspension (104  $\mu$ L stock solution, prepared as described above) was placed in a fluorimetric cell and diluted to 3040  $\mu$ L with the appropriate buffer solution (25 mM HEPES pH 7, 100 mM MCl with M = Li<sup>+</sup>, Na<sup>+</sup>, K<sup>+</sup>, Rb<sup>+</sup>, Cs<sup>+</sup>, or 100 mM NaX with X = F<sup>-</sup>, Cl<sup>-</sup>, Br<sup>-</sup>, I<sup>-</sup>). The total lipid concentration in the fluorimetric cell was 0.17 mM. An aliquot of MeOH solution of the ionophore (10-50  $\mu$ L of the appropriate mother solution in order to obtain the desired mol<sub>compound</sub>/mol<sub>lipid</sub> ratio) was then added to the lipid suspension and the cell was incubated at 25 °C for 30 min. HPTS emission was monitored at 510 nm and excitation wavelengths of 403 and 460 nm were used concurrently. After incubation, the time course of fluorescence was recorded for 200 s and then 50  $\mu$ L of 0.5 M MOH (with M = Li<sup>+</sup>, Na<sup>+</sup>, K<sup>+</sup>, Rb<sup>+</sup>, Cs<sup>+</sup> depending on the cation present in the extravesicular buffer solution) were rapidly added through an injector port and the fluorescence emission was recorded for 1200 s. Maximal changes in dye emission were obtained by final lysis of the liposomes with a detergent (40  $\mu$ L of 5% aqueous solution Triton® X-100). The extent of transport was calculated and normalized as previously described.

#### **Cell cultures and *in vitro* bioscreenings.**

Human MCF-7 breast adenocarcinoma cells, human neuroblastoma SH-SY5Y cell line, human prostate cancer DU145 cell line and human HaCaT keratinocytes were all purchased from ATCC (American Type Culture Collection, Manassas, Virginia, USA). MCF-7 and SH-SY5Y cells were grown in RPMI 1640 medium (Invitrogen, Paisley, UK), whereas DU145 and HaCaT cells were grown in DMEM (Invitrogen, Paisley, UK). Media were supplemented with 10% fetal bovine serum (FBS, Cambrex, Verviers, Belgium), L-glutamine (2 mM, Sigma, Milan, Italy), penicillin (100 units/ml, Sigma) and streptomycin (100  $\mu$ g/ml, Sigma), according to ATCC recommendations. The cells were cultured in a humidified air 95% carbon dioxide (CO<sub>2</sub>) 5% atmosphere at 37 °C.

The bioactivity of the guanine derivatives **Gua1** and **Gua2** was investigated through the estimation of a “cell survival index”, arising from the combination of cell viability evaluation with cell counting. Cells were inoculated in a 96-microwell culture plates at density of 10<sup>4</sup> cells/well and allowed to grow for 24 h. The medium was then replaced with fresh medium and cells were treated for further 48 h with a range of concentrations (1→100  $\mu$ M) of **Gua1** and **Gua2**. Cell viability was evaluated with the MTT assay procedure based on the redox ability of living mitochondria, which measures the level of mitochondrial dehydrogenase activity using the yellow 3-(4,5-dimethyl-2-thiazolyl)-2,5-diphenyl-2H-tetrazolium bromide (MTT, Sigma) as substrate [32]. Cell number was determined by TC10 automated cell counter (Bio-Rad, Milan, Italy), providing an accurate and reproducible total count of cells and a live/dead ratio in one step [33]. The calculation of the concentration required to inhibit the net increase in the cell number and viability by 50% (IC<sub>50</sub>) is based on plots of data carried out in triplicates and repeated three times. IC<sub>50</sub> values were obtained by means of a dose response curve by nonlinear regression using a curve fitting program, GraphPad Prism 5.0, and are expressed as mean  $\pm$  SEM.

#### **Statistical Analysis.**

All data were presented as mean  $\pm$  SEM. The statistical analysis was performed using Graph-Pad Prism (Graph-Pad software Inc., San Diego, CA) and ANOVA test for multiple comparisons was performed followed by Bonferroni's test.

## Acknowledgements.

We thank Centro di Metodologie Chimico-Fisiche (CIMCF), Università di Napoli “Federico II”, for the MS and NMR facilities.

## References.

- [1] O. Doluca, J. M. Withers, V. V. Filichev, Molecular engineering of guanine-rich sequences: Z-DNA, DNA triplexes, and G-quadruplexes, *Chem Rev.* 113 (2013) 3044-3083.
- [2] P. Murat, S. Balasubramanian, Existence and consequences of G-quadruplex structures in DNA, *Curr. Opin. Genet. Dev.* 25C (2014) 22-29.
- [3] T. M. Bryan, P. Baumann, G-quadruplexes: from guanine gels to chemotherapeutics, *Mol. Biotechnol.* 49 (2011) 198-208.
- [4] J. T. Davis, G. P. Spada, Supramolecular architectures generated by self-assembly of guanosine derivatives, *Chem. Soc. Rev.* 36 (2007) 296-313.
- [5] E. De Clercq, J. Neyts, Antiviral agents acting as DNA or RNA chain terminators. In *Antiviral Strategies*, Handb. Exp. Pharmacol. 2009; 189, Hans-Georg Kräusslich, Ralf Bartenschlager, Ed. Springer-Verlag Berlin Heidelberg, pp 53-84.
- [6] E. De Clercq, H. J. Field, Antiviral prodrugs - the development of successful prodrug strategies for antiviral chemotherapy, *Br. J. Pharmacol.* 147 (2006) 1-11.
- [7] For a recent review on acyclovir, see for example: R. A. Vere Hodge, H. J. Field, Antiviral agents for herpes simplex virus, *Adv. Pharmacol.* 67 (2013) 1-38.
- [8] For a recent review on ganciclovir, see for example: C. N. Kotton, CMV: Prevention, diagnosis and therapy, *Am. J. Transplant.* 13 (2013) 24-40.
- [9] For a recent review on entecavir, see for example: R. Sacco, Update on entecavir in the management of severe forms of Hepatitis B, *Hepat Med.* 4 (2012) 39-47.
- [10] L. P. Jordheim, D. Durantel, F. Zoulim, C. Dumontet, Advances in the development of nucleoside and nucleotide analogues for cancer and viral diseases, *Nat. Rev. Drug Discov.* 12 (2013) 447-464.
- [11] D. S. Gestó, N. M. Cerqueira, P. A. Fernandes, M. J. Ramos, Gemcitabine: a critical nucleoside for cancer therapy, *Curr. Med. Chem.* 19 (2012) 1076-1087.
- [12] C. M. Galmarini, J. R. Mackey, C. Dumontet, Nucleoside analogues and nucleobases in cancer treatment, *Lancet Oncol.* 3 (2002) 415-424.
- [13] P. Patel, E. Hanawa, R. Yadav, U. Samuni, C. Marzabadi, D. Sabatino, Synthesis, DNA binding and anti-leukemic activity of an aminoacyl nucleolipid, *Bioorg. Med. Chem. Lett.* 23 (2013) 5086-5090.
- [14] D. Musumeci, C. Irace, R. Santamaria, D. Montesarchio, Trifluoromethyl derivatives of canonical nucleosides: Synthesis and bioactivity studies, *Med. Chem. Comm.* 4 (2013) 1405-1410.
- [15] L. Simeone, D. Milano, L. De Napoli, C. Irace, A. Di Pascale, M. Boccalon, P. Tecilla, D. Montesarchio, Design, synthesis and characterisation of novel amphiphilic guanosine derivatives, *Chem. Eur. J.* 17 (2011) 13854-13865.
- [16] P. Prangkio, D. K. Rao, K. D. Lance, M. Rubinshtein, J. Yang, M. Mayer, Self-assembled, cation-selective ion channels from an oligo(ethylene glycol) derivative of benzothiazole aniline, *Biochim. Biophys. Acta*, 1808 (2011) 2877-2885.
- [17] R.-W. Wang, B. Gold, A facile synthetic approach to 7-deazaguanine nucleosides via a Boc protection strategy, *Org. Lett.*, 11 (2009) 2465-2468.
- [18] A. Porcheddu, G. Giacomelli, L. Piredda, M. Carta, G. Nieddu, A practical and efficient approach to PNA monomers compatible with Fmoc-mediated solid-phase synthesis protocols, *Eur. J. Org. Chem.* 34 (2008) 5786-5797.

- [19] G. Moiset, C. A. Lopez, R. Bartelds, L. Syga, E. Rijpkema, A. Cukkemane, M. Baldus, B. Poolman, S. J. Marrink, Disaccharides impact the lateral organization of lipid membranes, *J. Am. Chem. Soc.*, 136 (2014), 16167–16175.
- [20] T. Higashiyama, Novel functions and applications of trehalose, *Pure Appl. Chem.* 74 (2002) 1263–1269.
- [21] F. Berndt, M. Sajadi, N. P. Ernsting, R. Mahrwald, Covalent linkage of N-methyl-6-oxyquinolinium betaine to trehalose, *Carbohydr. Res.* 346 (2011) 2960–2964.
- [22] M. Adinolfi, L. De Napoli, G. Di Fabio, A. Iadonisi, D. Montesarchio, Modulating the activity of oligonucleotides: solid phase synthesis of sucrose-oligonucleotide hybrids, *Org. Biomol. Chem.* 2 (2004), 1879–1886.
- [23] J. D’Onofrio, M. de Champdoré, L. De Napoli, D. Montesarchio, G. Di Fabio, Glycomimetics as decorating motifs for oligonucleotides: solid phase synthesis, stability and hybridization properties of carbopeptoid-oligonucleotide conjugates, *Bioconjugate Chem.* 16 (2005) 1299–1309.
- [24] J. D’Onofrio, L. Petraccone, L. Martino, G. Di Fabio, A. Iadonisi, J. Balzarini, C. Giancola, D. Montesarchio, Synthesis, biophysical characterization and anti-HIV activity of glyco-conjugated G-quadruplex forming oligonucleotides, *Bioconjugate Chem.* 19 (2008) 607–616.
- [25] S. Licen, C. Coppola, J. D’Onofrio, D. Montesarchio, P. Tecilla, CyPLOS, a new family of synthetic ionophores, *Org. Biomol. Chem.* 7 (2009) 1060–1063.
- [26] C. Coppola, A. Paciello, G. Mangiapia, S. Licen, L. De Napoli, L. Paduano, P. Tecilla, D. Montesarchio, Design, synthesis and characterisation of a fluorescently labelled CyPLOS ionophore, *Chem Eur. J.* 16 (2010) 13757–13772.
- [27] L. Ma, W. A. Harrell, J. T. Davis, Stabilizing guanosine-sterol ion channels with a carbamate to urea modification in the linker, *Org. Lett.* 11 (2009) 1599–1602.
- [28] Y. P. Kumar, R. N. Das, S. Kumar, O. M. Scütte, C. Steinem, J. Dash, Triazole-tailored guanosine dinucleosides as biomimetic ion channels to modulate transmembrane potential, *Chem. Eur. J.* 20 (2014) 3023–3028.
- [29] N. Sakai, S. Matile, The determination of the ion selectivity of synthetic ion channels and pores in vesicles, *J. Phys. Org. Chem.* 19 (2006) 452–460.
- [30] B. Díaz de Greñu, P. Iglesias Hernández, M. Espona, D. Quiñonero, M. E. Light, T. Torroba, R. Pérez-Tomás, R. Quesada, Synthetic prodiginine Obatoclax (GX15-070) and related analogues: anion binding, transmembrane transport, and cytotoxicity properties, *Chem. Eur. J.* 17 (2011) 14074–14083.
- [31] F. Lang, E. K. Hoffmann, Role of ion transport in control of apoptotic cell death, *Compr. Physiol.* 2 (2012) 2037–2061.
- [32] F. Fiorito, C. Irace, A. Di Pascale, A. Colonna, G. Iovane, U. Pagnini, R. Santamaria, L. De Martino, 2,3,7,8-Tetrachlorodibenzo-p-dioxin promotes BHV-1 infection in mammalian cells by interfering with iron homeostasis regulation, *Plos One.* 8 (2013) e58845.
- [33] A. Lavecchia, C. Di Giovanni, C. Cerchia, A. Russo, G. Russo, E. Novellino, Discovery of a novel small molecule inhibitor targeting the frataxin/ubiquitin interaction via structure-based virtual screening and bioassays. *J Med Chem.* 56 (2013) 2861–2873.

## Graphical Abstract

A novel guanine analog with high ionophoric and antiproliferative activity

